Seventy-Meter Antenna Performance Predictions: GTD Analysis Compared With Traditional Ray-Tracing Methods

J. M. Schredder*

Ground Antenna and Facilities Engineering Section

A comparative analysis has been performed, using both the Geometrical Theory of Diffraction (GTD) and traditional pathlength error analysis techniques, for predicting RF antenna gain performance and pointing corrections. The NASA/JPL 70-meter antenna with its shaped surface was analyzed for gravity loading over the range of elevation angles. Also analyzed were the effects of lateral and axial displacements of the subreflector. Significant differences were noted between the predictions of the two methods, in the effect of subreflector displacements, and in the optimal subreflector positions to focus a gravity-deformed main reflector. The results are of relevance to future design procedure.

I. Introduction

Among a number of current trends in high performance antenna design is the replacement of paraboloid main reflectors and hyperboloid subreflectors with optimally shaped surfaces which provide uniform aperture illumination. Quantification of various RF gain loss mechanisms, especially those due to surface imperfections, is essential to understanding where cost-effective improvements might be realized. The traditional methods used for antenna gain and pointing analysis have been based on the assumption of paraboloid main reflectors and hyperboloid subreflectors. Newer methods

exist which deal with more general reflector shapes. One such method is implemented in the JPL Geometric Theory of Diffraction (GTD) program. This article compares gain and pointing predictions derived from traditional methods and GTD analysis under various conditions. The NASA/JPL 70-meter antenna, which has a shaped main reflector and a shaped subreflector, was used as a test sample. The effect of lateral and axial offsets of the subreflector was investigated along with the effect of gravity deformations of the main reflector with focusing of the subreflector.

II. Traditional Ray-Tracing Methods

For the analysis of gravity deformations of the main reflector, the traditional and GTD methods use the same set of nodal displacements, derived from a finite-element struc-

tural model. These are the X, Y, and Z (axial) components of symmetric unit-gravity-load deflections $(\Delta S_{symmetric})$ and antisymmetric unit-gravity-load deflections $(\Delta S_{antisymmetric})$. The two sets of deflections are combined according to the following equation:

$$\Delta S = \Delta S_{symmetric} \left[\sin{(EL_{rig})} - \sin{(EL)} \right]$$
$$+ \Delta S_{antisymmetric} \left[\cos{(EL_{rig})} - \cos{(EL)} \right] \tag{1}$$

where:

$$S = X, Y, \text{ or } Z$$

to yield the deflections at any desired elevation angle (EL). The rigging elevation angle (EL_{rig}) was arbitrarily set at 45 degrees.

In ray-tracing analysis, the half-pathlength errors are then fitted to a paraboloid by least squares, and the RMS of residuals of the fit is computed [1]. The deformed antenna is assumed to be perfectly focused. The RMS value is used in the Ruze equation [2] to compute the gain loss as follows:

$$\zeta = e \exp\left[-\left(\frac{4\pi(\text{RMS})}{\lambda} \right)^2 \right] \tag{2}$$

where:

ζ = efficiency

λ = wavelength

The elevation pointing shift due to gravity-loading main reflector and quadripod deflections is given by:

$$\theta = \theta_s [\sin{(EL_{rig})} - \sin{(EL)}] + \theta_{as} [\cos{(EL_{rig})} - \cos{(EL)}] \tag{3}$$

where θ_s is the pointing shift due to symmetrical gravity loading and θ_{as} is the pointing shift due to antisymmetric loading. For the 70-m antenna, $\theta_s = 0.0015$ degree and $\theta_{as} = 0.047$ degree.

This equation is derived from the finite element model and the best-fit paraboloid axis tilt. The fitting process also gives the parameters of the best-fit paraboloid, including its focus. The position of the subreflector vertex, the subreflector axis tilt, and the feedhorn phase center shift, as obtained from the whole antenna structure model, are combined with the main reflector best-fit geometry. A subreflector focusing offset

table is generated which brings the virtual image of the feed phase center into coincidence with the best fit main reflector focus [3]. This is shown in Fig. 1. The pointing shift predicted by Eq. (3) is added to the shift computed by Eq. (4) to derive a predicted net shift for the focused antenna.

Gain loss resulting from subreflector offsets is computed traditionally as follows. Data obtained from running the JPL Radiation Program [4] allowed the equivalent RMS pathlength error per unit subreflector displacement in lateral and axial directions to be expressed as functions of focal length to diameter ratio. For the shaped 70-meter antenna, the approximating f/D ratio is taken to be 0.389, which gives an RMS pathlength error of 0.0773 cm per centimeter of axial displacement and 0.0185 cm per centimeter of lateral displacement. These values are then used in the Ruze equation (Eq. [2]).

Pointing shift as a function of subreflector lateral displacement for a Cassegrain antenna is predicted by a simple geometric argument, given in [5]:

$$\theta = -\Delta Y \left(1 - \frac{1}{M}\right) \frac{K}{f} \tag{4}$$

where:

ΔY = lateral subreflector displacement

θ = pointing shift in radians

f = focal length

K = beam deviation factor

M = magnification factor

For the 70-m antenna, $f = 2722.9$ cm, M is estimated as 6.84, and K is estimated as 0.82.

III. The GTD Method

The GTD program evolved from an electric field integration program developed in 1978 and modified in 1983.[1] The program uses modified Jacobi polynomials to describe the radial dependence of the surface currents induced by the fields incident on the main reflector. The modified Jacobi polynomials are an orthogonal set with desirable convergence properties. The program uses two-dimensional Gauss integra-

[1] Y. Rahmat-Samii, "Offset Parabolic Reflector Computer Program for Analysis of Satellite Communications Antennas," JPL Publication D-1203 (internal document), Jet Propulsion Laboratory, Pasadena, California, December 1983.

tion to determine the coefficients for the eigenfunctions composed of the products of modified Jacobi polynomials and sine and cosine functions of the azimuth angle. These coefficients are then used in another series to compute the far-field electric field pattern.

The program described in JPL Publication D-1203[1] requires that the user supply subroutines to compute the following: a description of the main reflector surface that includes axial distance (Z) as a function of radius (r) and azimuth angle (ϕ), the first derivatives $\partial z/\partial r$, $\partial z/\partial \phi$, and the fields incident on the main reflector.

The GTD program represents the deformed or undeformed main reflector as a series of modified Jacobi polynomials added to a base paraboloid:

$$Z = \sum_n \sum_m (C_{nm} \cos n\phi + D_{nm} \sin n\phi) \, F_m^n \left(\frac{r}{R_{max}} \right) + z_0 + \frac{r^2}{4f}$$

(5)

where:

ϕ = azimuth angle

r = radius

R_{max} = the radius of the main reflector

f = focal length of base paraboloid

z_0 = arbitrary datum

The program computes two sets of electric and magnetic fields incident on the main reflector: a pair of fields reflected from the subreflector and a pair of fields diffracted from the subreflector. The reflected fields are computed using geometrical optics (GO), while the diffraction field is computed using the Geometrical Theory of Diffraction (GTD). The program in this form is documented in JPL Publication D-2583.[2]

IV. GTD Analysis of the 70-Meter Antenna

In this investigation, a number of modifications were made to the GTD program to accommodate the 70-meter antenna analysis. An additional data block was generated to provide storage for Jacobi polynomial coefficients for both the shaped subreflector and the deformed main reflector (previously, the

[2] T. Veruttipong, et al., "Dual Shaped and Conic GTD/Jacobi-Bessel Analysis Programs," JPL Publication D-2583 (internal document), Jet Propulsion Laboratory, Pasadena, California, July 30, 1985.

program could analyze one or the other, but not both). Also, a change was made in the sequence in which Jacobi polynomial values were computed and stored and provided a major increase in execution speed.

Analysis of a gravity-deformed reflector involves the following five steps:

(1) The computation of node deflections at a given elevation angle is the same as in the conventional analysis, and the deflections (u, v, w) are added to the node coordinates (x, y, z) for an undeflected reflector to arrive at a set of deflected nodes. The 70-meter model that was used has 764 nodes for a half-model.

(2) A grid of axial positions $z(r, \phi)$ at evenly spaced values of radius (r) and azimuth angle (ϕ) is generated. The radius varies from zero at the center to R_{max}, the radius of the main reflector, and the azimuth angle varies from 0 to 360 degrees. To generate the grid, a set of nine neighboring nodes around each grid point is used, as shown in Fig. 2. First, three interpolating parabolas along points 1-2-3, 4-5-6, and 7-8-9 are computed. These parabolas are evaluated at the grid point radius to give three values of azimuth angle and Z at this radius. Then a fourth interpolating parabola is computed giving Z as a function of angle. This parabola is evaluated at the grid point angle to yield the interpolated Z value. Typical grid spacing was 416 intervals in radius and 256 intervals in angle.

(3) The following equation is integrated by standard numerical methods to generate the Jacobi polynomial coefficients (C_{nm}, D_{nm}) which describe the reflector surface:

$$C_{nm} = \frac{\epsilon_n}{2\pi} \int_0^{2\pi} \int_0^1 \cos n\phi \, F_m^n(s) \, s \, d\phi \, ds$$

(6)

$$D_{nm} = \frac{\epsilon_n}{2\pi} \int_0^{2\pi} \int_0^1 \sin n\phi \, F_m^n(s) \, s \, d\phi \, ds$$

where:

$s = r/R_{max}$

$\epsilon_n = 1$ if $n = 0$

$\epsilon_n = 2$ if $n \neq 0$

To represent the gravity-deformed main reflector shapes, a 7 X 25 set of coefficients was used $(n = 0,$

1, ..., 6; $m = 0, 1, ..., 24$), which can model 24 ripples in radius and 6 cycles in azimuth angle.

(4) To check the accuracy of the Jacobi polynomial fit, the reflector surface is reconstructed from the Jacobi polynomial representation (at the node radii and angles). To do this, the coefficients determined in step 3 are entered into Eq. (5). The computed Z values are compared with the Z values derived from the finite element model. For gravity deformations, RMS differences of 0.075 mm (0.003 inch) to 0.175 mm (0.005 inch) were found. These differences were much smaller than the gravity deformations.

(5) The coefficients determined in step 3 are also used to represent the deformed main reflector in the GTD program.

Figure 3 shows the sequence of computations of both the traditional and GTD methods.

The Jacobi polynomial representation of the undeflected main reflector consists of a set of 15 coefficients ($n = 0$; $m = 0, 1, ..., 14$) of polynomials in radius, as there is no angular dependence of the ideal reflector surface. The first 15 Jacobi polynomials were sufficient to describe the deviation of the radial profile from a parabola. This representation of the "perfect" reflector was used in two ways: (1) to generate the undeflected node positions for the gravity deformation analysis; and (2) to study the effects of subreflector displacements.

Among the input variables to the GTD program are the subreflector and feed positions; the orientations of the main reflector, subreflector, and feed coordinate systems; and the RF wavelength. The frequency used in this study was 8.45 GHz, which has a wavelength of 35.48 mm (1.397 in.). The study was performed with the subreflector pointed at the X-band horn, as shown in Figs. 4 and 5. The geometry is shown in more detail in JPL Publication D-1843.[3]

V. Results

The following results are compared between GTD and traditional analysis:

(1) Gain loss resulting from subreflector lateral and axial offsets, and pointing shift due to lateral offsets.

(2) Gain loss and pointing shift as functions of elevation angle with the subreflector focused.

(3) Prediction of best subreflector offsets to focus a gravity-deformed antenna as a function of elevation angle.

It should be noted that the subreflector offsets are given in units of the wavelength at 8.45 GHz.

Figure 6 shows gain loss for a perfect main reflector as a function of axial subreflector displacement predicted by the two methods. For positive axial displacements (away from the main reflector) the agreement is very close, but the difference between the two curves is sizable for negative displacements.

Table 1 shows the gain loss predicted by the two methods for lateral subreflector displacements, while Table 2 shows the pointing shift predicted. There is a large difference in the predicted gain loss; however, both methods predict a square-law dependence of gain loss on lateral subreflector displacement. Also, the pointing shift predicted is somewhat different. Ray-tracing methods predict a shift of 0.01472 degree per centimeter of lateral displacement, while GTD predicts 0.01346 degree per centimeter of lateral displacement.

Figures 7 and 8 show the predicted gain loss and pointing shift, respectively, of the 70-meter antenna with focused subreflector as functions of elevation angle. For each figure, three sets of curves were generated: (1) predictions from traditional methods; (2) predictions from GTD analysis using the subreflector focusing tables furnished by traditional methods; and (3) predictions from GTD analysis with subreflector position varied to maximize the predicted gain. If the gain is maximized by varying the subreflector position, the gain loss predictions of GTD analysis agree with those of ray-tracing analysis to within a few hundredths of a decibel. This is considered good agreement.

Figure 9 contains four curves. The two broken lines represent the subreflector offsets required to bring the virtual image of the feed phase center into coincidence with the focus of the best-fit paraboloid, while the two solid lines represent the results of searching for the subreflector positions which maximize the gain predicted by GTD analysis. Note that in both cases, the offsets are measured from the original position of the subreflector, in the main reflector coordinate system. The agreement appears to be good in Z and poor in Y.

[3] A. G. Cha and W. A. Imbriale, "Computer Programs for the Synthesis and Interpolation of 70-m Antenna Reflector Surfaces," JPL Publication D-1843 (internal document), Jet Propulsion Laboratory, Pasadena, California, November 1984.

VI. Conclusion

The predictions of traditional ray tracing and GTD analysis have been compared in this article for subreflector displacements and for the focused, gravity-deformed 70-meter antenna. There is a significant difference in the gain loss predicted by the two methods for axial subreflector displacement, and a large difference in the gain loss predicted for lateral displacement. The pointing shift predicted for lateral displacement is also somewhat different.

For the focused gravity-deformed antenna, the gain loss predictions of the two methods show good agreement if the subreflector position is varied to maximize the gain. It is noteworthy that the pointing shift predictions show close agreement between ray tracing and GTD analysis if the traditional subreflector focusing method is used. However, if the traditional method of determining subreflector focusing offsets is used, the agreement for gain loss predictions is poor. This study shows significant differences between the subreflector offsets that align the virtual image of the feed phase center with the best-fit paraboloid focus and the offsets which maximize the gain. Past studies have indicated that aligning the main focus and feed phase center will yield good results in maximizing the gain of paraboloid-hyperboloid systems. The present results indicate that methods which compute the electric and magnetic fields are required to give good results when dealing with shaped surfaces.

References

[1] M. S. Katow and L. W. Schmele, *Antenna Structures: Evaluation Techniques of Reflector Distortions*, JPL Space Programs Summary No. 37-40, vol. IV, Jet Propulsion Laboratory, Pasadena, California, August 31, 1966.

[2] J. Ruze, "Physical Limitations on Antenna," Technical Report 248, Cambridge, Massachusetts: Research Laboratory of Electronics, Massachusetts Institute of Technology, October 1952.

[3] R. D. Hughes and M. S. Katow, "Subreflector Focusing Techniques Applied to New DSS-15 and DSS-45 34-Meter Antennas," *TDA Progress Report 42-80*, vol. October–December 1984, Jet Propulsion Laboratory, Pasadena, California, pp. 832–890, February 15, 1984.

[4] M. S. Katow, "Thirty-four-Meter Antenna-Subreflector Translations to Maximize RF Gain," *DSN Progress Report 42-62*, vol. January–February 1981, Jet Propulsion Laboratory, Pasadena, California, pp. 112–120, April 15, 1981.

[5] R. Levy, "Optimization of Antenna Structure Design," presented at the Eighth ASCE Conference on Electronic Computation, Houston, Texas, February 1983.

Table 1. Comparison of predictions of gain loss caused by subreflector lateral displacements

Lateral displacement	Gain loss, dB (traditional)	Gain loss, dB (GTD)
λ^* in $+Y$ direction	0.23	0.55
$\frac{\lambda}{2}$ in $+Y$ direction	0.06	0.14
λ in $-Y$ direction	--	0.56
λ in $+X$ direction	--	0.56

$^*\lambda$ = 3.548 cm (1.397 in.) at 8.45 GHz.

Table 2. Comparison of predictions of pointing shift caused by subreflector lateral displacements

Lateral displacement	Pointing shift (traditional), deg	Pointing shift (GTD), deg
λ^* in $+Y$ direction	0.05228	0.04776
$\frac{\lambda}{2}$ in $+Y$ direction	--	0.02388
λ in $-Y$ direction	--	0.04775
λ in $+X$ direction	--	0.04775

$^*\lambda$ = 3.548 cm (1.397 in.) at 8.45 GHz.
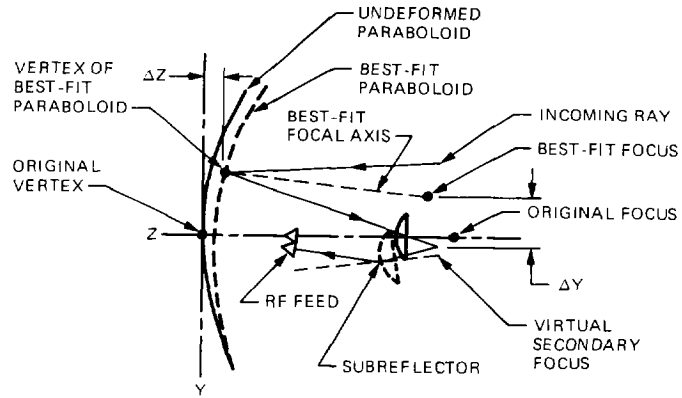
Fig. 1. RF center ray tracing and hyperboloid offsets with gravity distortions
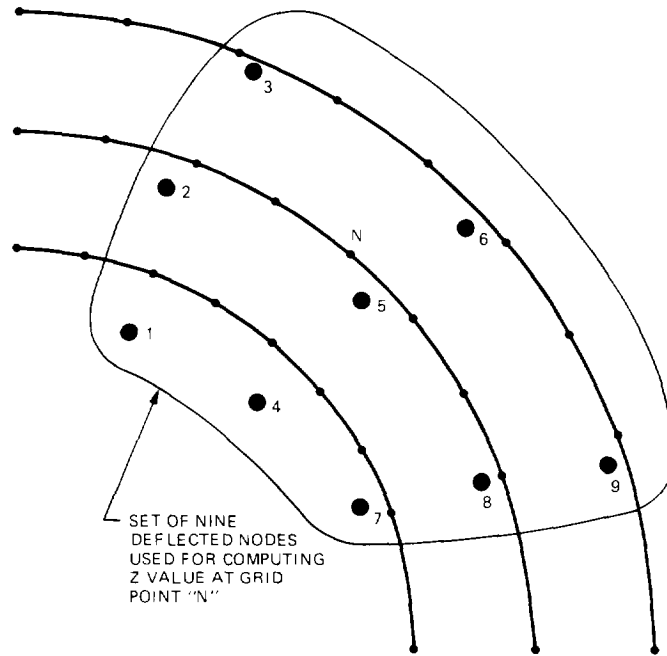
Fig. 2. Use of deflected node coordinates to compute axial (Z) coordinate of a grid point
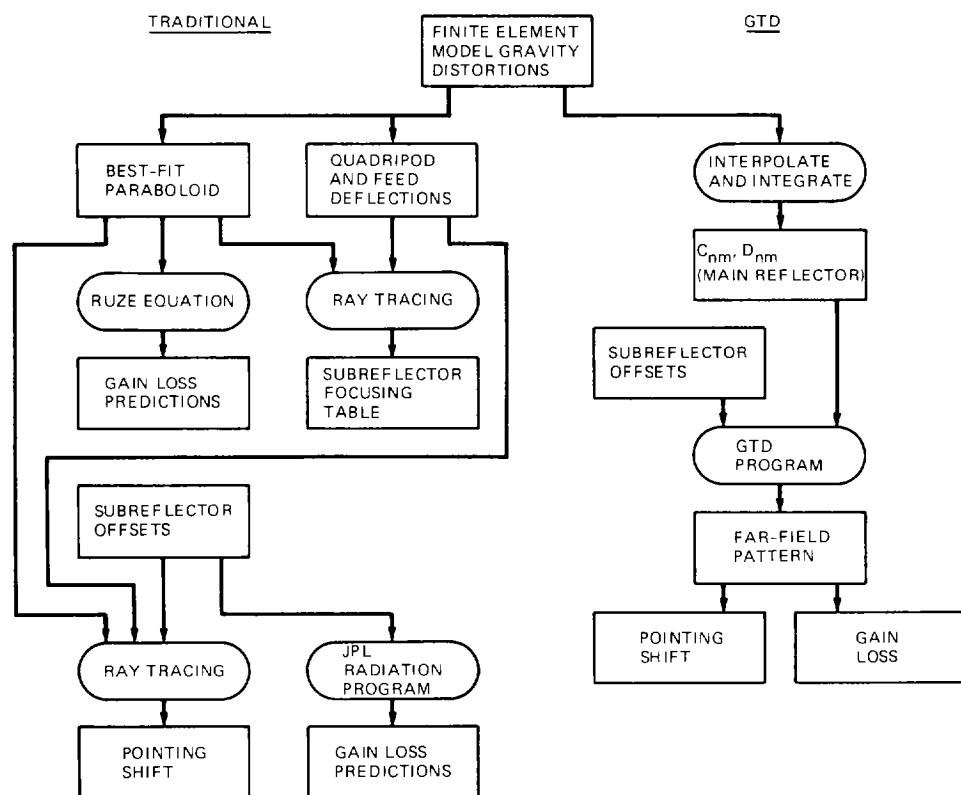
Fig. 3. Sequence of computations for calculating effects of gravity deformations and subreflector offsets by traditional and GTD methods
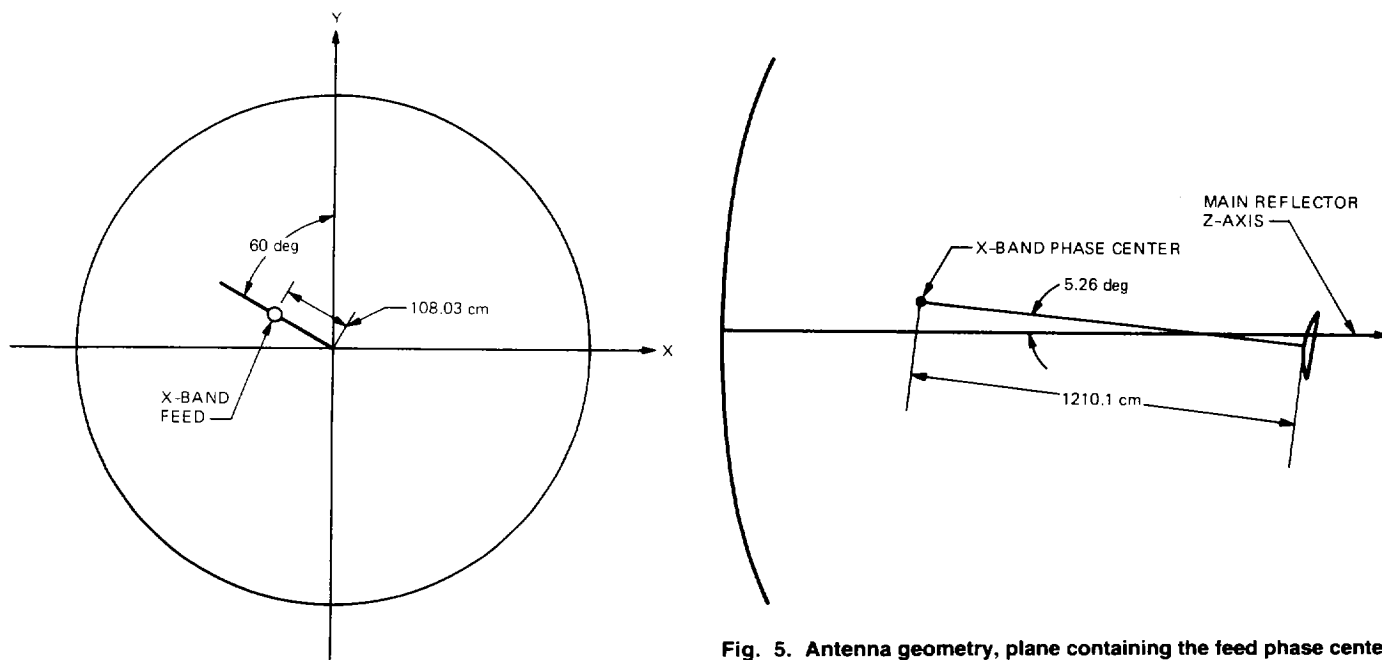

Fig. 4. Antenna geometry used in this study, looking into main reflector from space

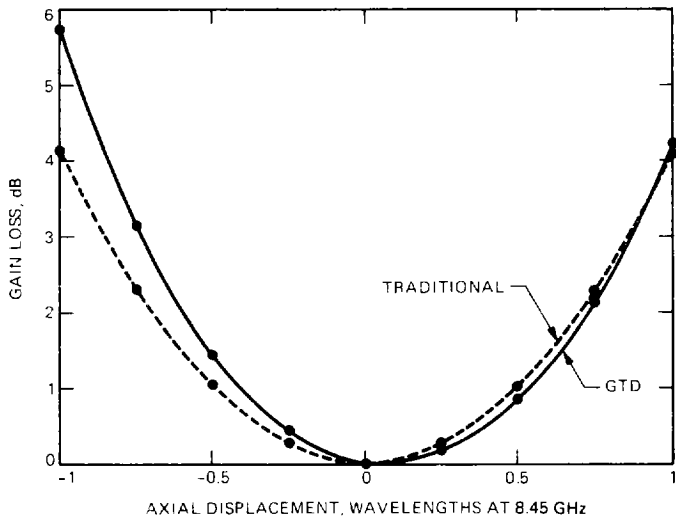Fig. 5. Antenna geometry, plane containing the feed phase center and the main reflector Z axis
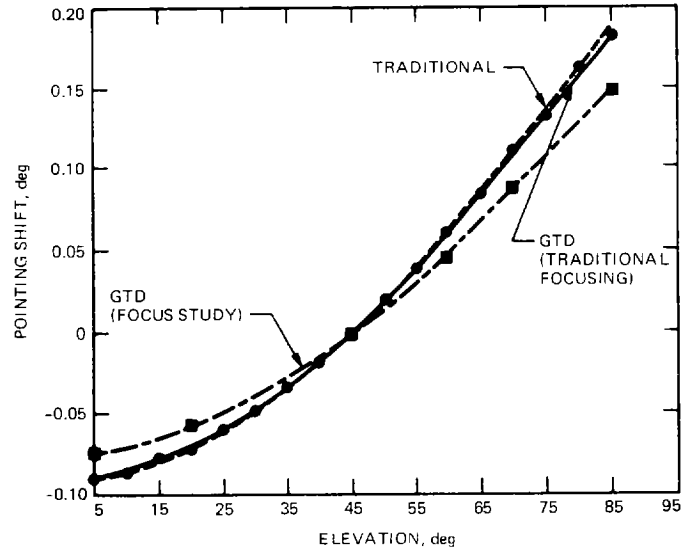
Fig. 6. Gain loss versus axial subreflector displacement

Fig. 8. Elevation pointing shift versus elevation for gravity-deformed, focused antenna
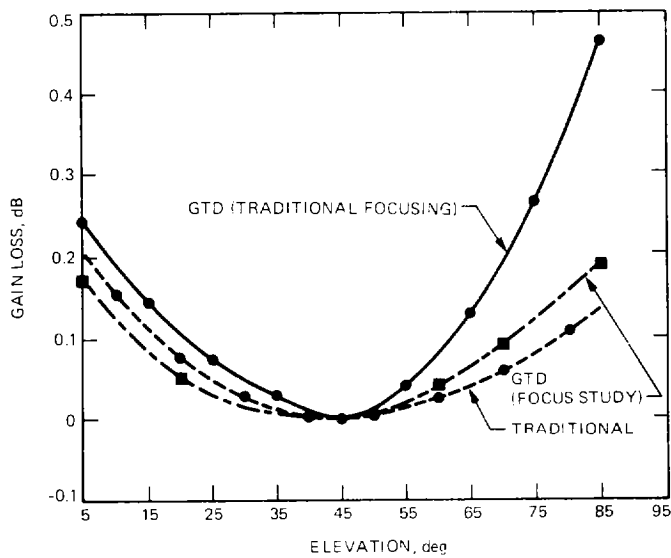

Fig. 7. Gain loss versus elevation for gravity-deformed, focused antenna
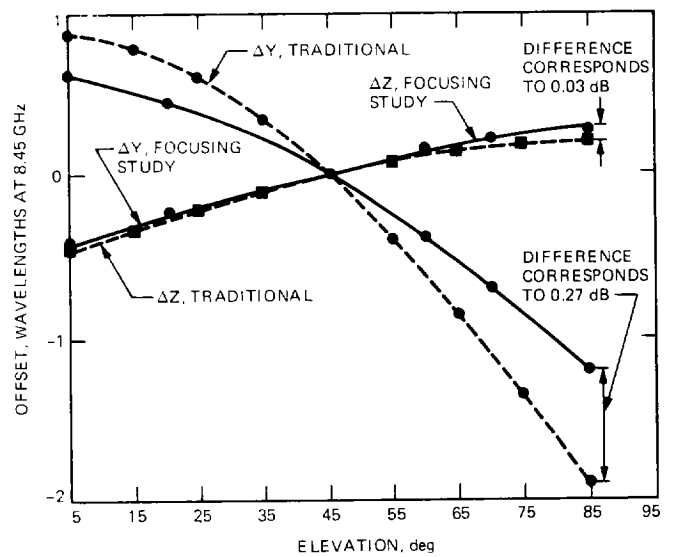

Fig. 9. Subreflector lateral and axial offsets to focus a gravity-deformed 70-meter antenna